

# Design, synthesis and biological evaluation of 4-piperidin-4-yl-triazole derivatives as novel histone deacetylase inhibitors

He Miao<sup>1,2,§</sup>, Jianjun Gao<sup>2,§</sup>, Zishuo Mou<sup>2</sup>, Baolei Wang<sup>2</sup>, Li Zhang<sup>1</sup>, Li Su<sup>1</sup>, Yantao Han<sup>3,\*</sup>, Yepeng Luan<sup>1,\*</sup>

<sup>1</sup>Department of Medicinal Chemistry, School of Pharmacy, Qingdao University, Qingdao, Shandong, China;

<sup>2</sup>Department of Pharmacology, School of Pharmacy, Qingdao University, Qingdao, Shandong, China;

<sup>3</sup>Department of Pharmacology, College of Basic Medicine, Qingdao University, Qingdao, Shandong, China.

## Summary

Histone deacetylase is an important member of epigenetics and a well validated target for anti-cancer drug discovery. In this study, we designed and synthesized a series of twenty-one novel hydroxamic acid-based histone deacetylase inhibitors with 4-piperidin-4-yl-triazole as the core skeleton. Most target compounds displayed excellent inhibition rates toward histone deacetylases at the concentration of 1  $\mu$ M. Among them, the inhibition rates of two compounds MH1-18 and MH1-21 exceeded 90%. Furthermore, these two compounds selectively inhibited the activity of histone deacetylase 6 with low IC<sub>50</sub> values. The high potency of them toward histone deacetylase 6 was rationalized by molecular docking studies. We found that MH1-18 and MH1-21 moderately inhibited the proliferation of four human cancer cell lines SGC-7901, NCI-H226, MCF-7, and HL-60. However, MH1-21 showed potent efficacy in suppressing the migration of MCF-7 cells. Results obtained in the current study shed light on designing potent HDAC6 inhibitors as anti-cancer agents.

**Keywords:** Histone deacetylase, isoform, selective, inhibitor, anti-tumor

## 1. Introduction

Acetylation as one of the most important covalent modification manners in the field of epigenetics, the level of it is taken control of by two families of enzymes with opposite mechanisms, histone acetyltransferases (HATs) and histone deacetylases (HDACs). HDACs are responsible for removal of the acetyl group from lysine residues in histones and non-histone substrates (1). Till now, 18 isoforms of HDACs have been discovered, and they are divided into four categories based on their sequence similarity and functions: class I (HDAC1, 2,

3 and 8), class II (class IIa (HDAC4, 5, 7 and 9) and class IIb (HDAC6 and 10)) and class IV (HDAC11) are all zinc-dependent HDACs, while class III HDACs are NAD<sup>+</sup>-dependent (2-4). Studies demonstrated that HDACs are key enzymes regulating important cell processes such as cell-cycle progression and apoptosis (2-4).

Overexpression of HDAC is involved in many cancers, so HDAC has become an important target in the development of anti-cancer drugs (5-9). A large number of HDAC inhibitors (HDACis) have been reported and some of them have been approved by FDA such as vorinostat (SAHA), romidepsin, belinostat, panobinostat, and chidamide (10-12). Pan-HDACis as the majority of reported HDACis often cause some adverse effects, such as fatigue, nausea, vomiting, and cardiotoxicity (13-15) which greatly limit their application in cancer therapy. To avoid these adverse effects and enhance the efficacy against solid tumors, more and more researches are concentrating on the development of isoform selective HDACis, especially HDAC6 selective inhibitors which usually cause less toxicities. Different from other HDAC isoforms,

Released online in J-STAGE as advance publication April 25, 2019.

<sup>§</sup>These authors contributed equally to this work.

\*Address correspondence to:

Dr. Yantao Han, Department of Pharmacology, College of Basic Medicine, Qingdao University, Qingdao 266071, China.  
E-mail: hanyt@qdu.edu.cn

Dr. Yepeng Luan, Department of Medicinal Chemistry, School of Pharmacy, Qingdao University, Qingdao 266021, Shandong, China.

E-mail: yluan@qdu.edu.cn

HDAC6 is located in the cytoplasm and mainly responsible for deacetylating non-histone substrates such as  $\alpha$ -tubulin, cortactin, HSP90, and other proteins (16,17). HDAC6 is involved in many cellular processes such as misfolded protein degradation, cell adhesion, cell migration, cell growth, immune synapse formation and stress granule formation (18,19). Several selective HDAC6 inhibitors have been extensively explored due to their relatively low toxicity compared with pan-HDACis (4,20). ACY1215, a well-known and moderately selective HDAC6 inhibitor with 10- to 12-fold selectivity over class I HDACs, is now in phase I/II clinical trials in combination with dexamethasone and bortezomib, lenalidomide, or pomalidomide for the treatment of multiple myeloma (21-23).

In this work, we designed and synthesized novel HDAC6 selective inhibitors utilizing 4-piperidin-4-yl-triazole fragment as the backbone. Enzyme inhibition activity, antiproliferative activity, anti-migration activity and their proposed binding modes with HDAC6 were all investigated.

## 2. Materials and Methods

### 2.1. Chemistry

All chemical reagents and solvents were purchased from Energy Chemical (Shanghai, China), and used as received without any purification. Thin-layer chromatography was performed on 0.20 mm Silica Gel 60 F254 plates (Qingdao Haiyang Chemical, China). MS spectra were acquired on a Thermo Scientific LTQ Orbitrap XL mass spectrometer. <sup>1</sup>H NMR spectra, and <sup>13</sup>C NMR spectra were acquired on a Bruker DRX 400 NMR spectrometer using CDCl<sub>3</sub> or DMSO-d<sub>6</sub> as solvent. Chemical shifts were reported in parts per million (ppm,  $\delta$ ) relative to the solvent peak (<sup>1</sup>H, CDCl<sub>3</sub>  $\delta$  7.26 ppm, DMSO-d<sub>6</sub>  $\delta$  2.50 ppm; <sup>13</sup>C, CDCl<sub>3</sub>  $\delta$  77.0 ppm, DMSO-d<sub>6</sub>  $\delta$  39.6 ppm). Coupling constants (*J*) were measured in hertz (Hz).

### 2.2. Cell line and cell culture

Human cancer cell lines SGC-7901 (gastric cancer), NCI-H226 (lung squamous cell cancer), MCF-7 (breast cancer), and HL-60 (leukemia) were obtained from China Cell Bank (Shanghai, China) and maintained in RPMI-1640 supplemented with 10% fetal bovine serum (FBS; PAN Biotech) at 37°C in a humid atmosphere (5% CO<sub>2</sub>-95% air).

### 2.3. In vitro HDAC inhibition fluorescence assay

In brief, 10  $\mu$ L of enzyme solution (HeLa cell nuclear extract, HDAC1, or HDAC6) was mixed with different concentrations of tested compounds (50  $\mu$ L). The mixture was incubated at 37°C for 5 min, followed by

adding 40  $\mu$ L fluorogenic substrate (Boc-Lys(acetyl)-AMC). After incubation at 37°C for 30 min, the mixture was quenched by addition of 100  $\mu$ L of developer containing trypsin and trichostatin A (TSA). Over another incubation at 37°C for 20 min, fluorescence intensity was measured using a microplate reader at excitation and emission wavelengths of 390 and 460 nm, respectively. The inhibition rates were calculated from the fluorescence intensity readings of tested wells relative to those of control wells, and the IC<sub>50</sub> values were calculated using a regression analysis of the concentration/inhibition data.

### 2.4. In vitro antiproliferative activity assay

The antiproliferative activities of the compounds were tested in four human cancer cell lines SGC-7901 (gastric cancer), NCI-H226 (lung squamous cell cancer), MCF-7 (breast cancer), and HL-60 (leukemia). Cells in logarithmic phase were seeded in 96-well plates and allowed to adhere (except for HL-60). Then the cells were incubated with indicated concentrations of the compounds for 72 h. 3-(4,5-Dimethylthiazol-2-yl)-2,5-diphenyltetrazolium bromide (MTT) was subsequently added for an extra 3 h of incubation. The MTT formazan precipitate was dissolved in DMSO, and the absorbance was measured at a wavelength of 570 nm by a Spectramax M5 microtiter plate luminometer (Molecular Devices, Sunnyvale, CA, USA) (24-26). Experiments were performed in triplicate and repeated for three times.

### 2.5. Wound healing assay

MCF-7 cells were seeded in 6-well plates at a density of 10<sup>6</sup> cells/well and allowed to reach 100% confluence. After treatment with mitomycin C (10  $\mu$ g/mL, 12 h), a scratch wound was created on the cell surface using a 200- $\mu$ L pipette tip. The detached cells were washed away with PBS. The medium was changed to serum free RPMI-1640 with the representative compound (at three concentrations), and the cells were continuously cultured for 48 h. The wound was photographed with an inverted phase contrast microscope (Nikon; magnification, 40 $\times$ ) at 0, 12, 24, 36, and 48 h. The migration distance and areas were calculated using ImageJ.

### 2.6. Docking study

Compounds were docked into the active site of HDAC6 (PDB entry: 5WGL) using Tripos SYBYL-X 2.1. Before docking process, the protein structure retrieved from PDB site was treated by deleting water molecules, FF99 charges. A 100-step minimization process was performed to further optimize the protein structure. The molecular structures were generated with Sybyl/Sketch

module and optimized using Powell's method with the Tripos force field with convergence criterion set at 0.05 kcal/(Å mol) and assigned charges with the Gasteiger\_Hückel method (27). Molecular docking was carried out via the Sybyl/SurflexDock module. Other docking parameters were kept to the default values.

### 2.7. Statistical analysis

Data were expressed as mean for at least three different determinations. Statistical significance was analyzed by one-way analysis of variance (ANOVA) followed by Dunnett's multiple range tests. The value of  $p < 0.05$  was considered as statistically significant. Statistical analysis was performed using the SPSS/Win 16.0 software (SPSS, Inc, Chicago, IL, USA).

## 3. Results and Discussion

### 3.1. Chemistry

The structures of all 21 target compounds and the synthetic route were showed in Scheme 1. In general, the canonical pharmacophore of a HDACi is composed of three parts: a cap structure that can interact with the rim of the entrance of the active pocket of HDACs, a zinc ion ( $Zn^{2+}$ ) binding group (ZBG), and a linker responsible for the connection of cap and ZBG and for interaction with the hydrophobic tunnel of the active site (28). In this work, we designed and synthesized novel HDAC6 selective inhibitors utilizing 4-piperidin-4-yl-triazole fragment as core skeleton and the cap part. Actually, many HDACis containing a triazole moiety were reported due to its structural stability. Triazole is relatively resistant to metabolic degradation and can perform as an bioisostere of esters and amides (29). Hydroxamic acid was selected as the ZBG due to its strong affinity with  $Zn^{2+}$ .

The organic synthesis work started with the commercially available 1-Boc-4-hydroxypiperidine which was allowed to react with methanesulfonyl chloride (MsCl) in presence of triethylamine (TEA) to give the methanesulfonyl ester **1**. And the methanesulfonyl ester was substituted by sodium azide ( $NaN_3$ ) to give the azido intermediate **2**. In another hand, the methyl 6-propionamidohexanoate **3** was obtained by the condensation of methyl 6-aminocaproate hydrochloride and propionic acid in the presence TEA and dicyclohexylcarbodiimide (DCC). Then compound **3** was allowed to react with compound **2** through Click reaction to give the methyl ester compound **4**. After deprotection mediated by trifluoroacetic acid (TFA), the important derivative **5** was obtained and allowed to react with different aryl acid to give the compounds **6-1** to **6-21**. Finally, in the presence of  $NH_2OH$  in anhydrous methanol, the hydroxamic acid final products **MH1-1** to **MH1-21** possessing different substituent groups were

obtained. Specific synthetic procedures and spectroscopy data of all compounds see supplementary data (<http://www.biosciencetrends.com/action/getSupplementalData.php?ID=42>).

### 3.2. In vitro anti-HDACs activity

We first screened the inhibitory activity of all 21 final products against Hela cell nucleus extracts whose main component is class I HDACs. Single concentration (1  $\mu M$ ) was used and the inhibition rate (%) was calculated. The results were showed in Figure 1. All 21 compounds displayed moderate to strong inhibitory activities against HDACs demonstrating that the 4-piperidin-4-yl-triazole fragment as the "cap" part and the linker length were desirable. Among all compounds, five ones (MH1-2, MH1-5, MH1-14, MH1-18, and MH1-21) displayed potent inhibitory activity against HDACs with the inhibition rate higher than 80% at 1  $\mu M$ . The cap part structures of MH1-2, MH1-5, MH1-18, and MH1-21 all contained polar atoms such as oxygen, fluoride and nitrogen which may contribute to the interactions with HDACs. Notably, the inhibition rates of compounds MH1-18 and MH1-21 were 93.6% and 92.7%, respectively, comparable to that of SAHA (96.3%).

### 3.3. HDAC isoform specificity of compounds MH1-18 and MH1-21

With two potent compounds MH1-18 and MH1-21 in hand, the isoform selectivity of them was further evaluated. HDAC1 (class I) and HDAC6 (class IIb) were selected as the targets, SAHA and HDAC6 selective inhibitor ACY1215 were utilized as the positive controls. The result was showed in Table 1. Consistent with published data, SAHA as a pan HDACi was almost equipotent toward HDAC1 and 6 without conspicuous selectivity. While, ACY1215 as a well-studied HDAC6 selective inhibitor displayed high potency to HDAC6 with the  $IC_{50}$  value of 8.0 nM, and the SF (6/1) (selectivity factor for HDAC6 over HDAC1) was 9.1. Encouragingly, our two inhibitors MH1-18 and MH1-21 were also robust HDAC6 inhibitors with the  $IC_{50}$  values of 11.5 and 8.6 nM, respectively. And the SF (6/1) values were discernible (10.4 and 12.3, respectively), even slightly better than that of ACY1215.

### 3.4. In vitro antiproliferative activity of compounds MH1-18 and MH1-21

Since compounds MH1-18 and MH1-21 had the best HDACs inhibitory activity, they were evaluated in an MTT assay to determine their antiproliferative effect on human cancer cell line SGC-7901 (gastric cancer), NCI-H226 (lung squamous cell cancer), MCF-



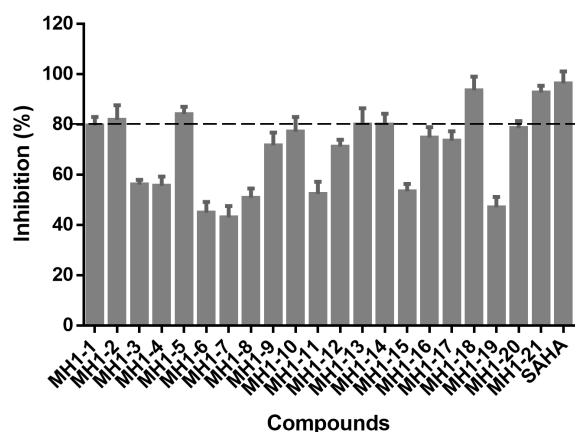


Figure 1. The inhibition rates of all 21 compounds against HDACs at 1  $\mu$ M concentration.

Table 1. Inhibitory activity of four representative compounds toward HDAC1 and 6

Compound	IC <sub>50</sub> <sup>a</sup> , nM		SF(6/1) <sup>b</sup>
	HDAC1	HDAC6	
MH1-18	119.2	11.5	10.4
MH1-21	105.6	8.6	12.3
SAHA	43.2	20.7	2.1
ACY1215	73.0	8.0	9.1

<sup>a</sup>The IC<sub>50</sub> values are the means of three experiments. <sup>b</sup>SF(6/1): selectivity factor for HDAC6 over HDAC1. SF(6/1) = IC<sub>50</sub>(HDAC1)/IC<sub>50</sub>(HDAC6).

Table 2. Antiproliferative effects on four tumor cell lines

Compound	IC <sub>50</sub> <sup>a</sup> , nM			
	SGC-7901	NCI-H226	MCF-7	HL-60
MH1-18	N.D.	N.D.	N.D.	57.7
MH1-21	166.3	119.3	226.4	43.8
ACY1215	10.2	7.44	6.31	6.73
SAHA	5.8	5.41	7.10	3.87

<sup>a</sup>IC<sub>50</sub> values are the mean of at least three experiments. N.D., not determined.

7 (breast cancer), and HL-60 (leukemia). Treatment with our two compounds as well as the positive control SAHA and ACY1215 for 72 h resulted in dose-dependent growth inhibition of all four cancer cell lines (Table 2). Contrast to the strong enzyme inhibitory activity, our two compounds MH1-18 and MH1-21 showed moderate activity in suppressing the cell proliferation, with IC<sub>50</sub> values more than 40  $\mu$ M for the four cancer lines. This result is consistent with the low antiproliferative activity of many known selective HDAC6 inhibitors (20,30). For example, in our previous work, we designed and synthesized three novel HDAC6 inhibitors LYP-2, -3, and -6 with the 4-aminopiperidine-1-carboxamide as the core structure which showed moderate efficacy in suppressing the proliferation of cancer cells (20). In another study, HDAC6 selective inhibitor 4-hydroxybenzoic acid failed to induce significant cell death in MCF-7 cells

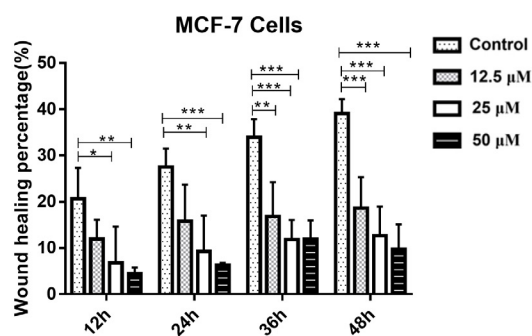
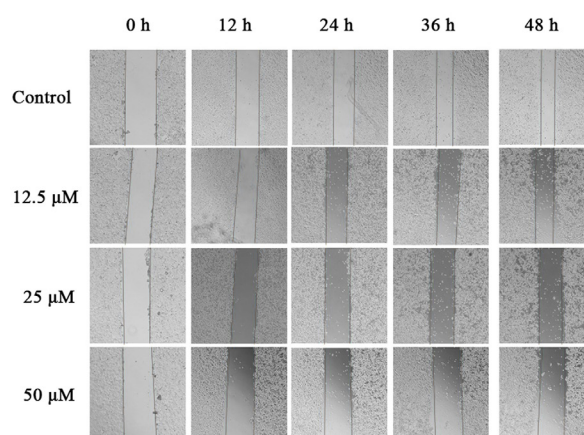
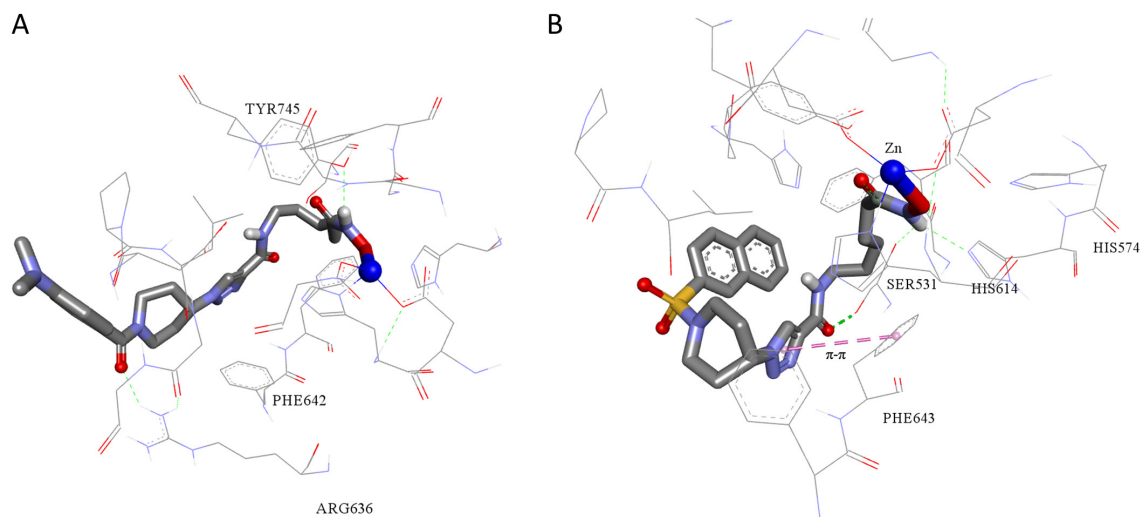


Figure 2. MH1-21 suppressed migration of MCF-7 cells. The effect of MH1-21 on MCF-7 tumor cell migration was determined using a wound healing assay. The cells were exposed to 12.5, 25, or 50  $\mu$ M of MH1-21 for 12, 24, 36, and 48 h, respectively, and the wound areas were measured at each time point. \* $p$  < 0.05, \*\* $p$  < 0.01, \*\*\* $p$  < 0.001 vs. control.

at concentrations below 20  $\mu$ M (30). On the other hand, the relatively low antiproliferation activity of MH1-18 and MH1-21 may possibly be attributed to their high polarity, as the calculated LogP (cLogP) values of MH1-18 and MH1-21 were -1.03 and 0.40 (by ChemDraw 14.0), respectively. While the cLogP values of ACY1215 and SAHA were 3.38 and 0.989. The permeability across the cell membrane of our compounds might be further improved.

### 3.5. Compound MH1-21 suppressed the migratory capability of MCF-7 tumor cells

As reported, HDAC6 plays a significant role in migration of tumor cells (31), in this work, we tested the anti-migration activity of compound MH1-21 which displayed best inhibitory activity toward HDAC6 with good selective index. To investigate the anti-migration effect of MH1-21, an *in vitro* wound healing assay was performed using MCF-7 cells. Results were showed in Figure 2, which indicated that treatment with three concentrations of MH1-21 (12.5, 25 and 50  $\mu$ M) all remarkably reduced the migratory capability of MCF-7 cells compared to that of the blank control group at 12, 24, 36 and 48 h after wound creation. This result suggested that compound MH1-21 possessing potent



**Figure 3.** Proposed binding model of compounds MH1-18 (A) and MH1-21 (B) with HDAC6 (derived by modification of PDB code 5WGL using Tripos SYBYL-X 2.1). The  $Zn^{2+}$  is shown as a blue sphere. Hydrogen bonds are shown as green dashed lines. The figure was generated by Discovery Studio Visualizer.

inhibitory activity toward HDAC6 was able to inhibit the migration of MCF-7 cells.

### 3.6. The docking results of compound MH1-18 and MH1-21 to HDAC6

Considering that compound MH1-18 and MH1-21 displayed potent inhibitory activity toward HDAC6, we investigated the proposed binding modes of these two compounds with HDAC6 (Figure 3). The crystal structure of *Danio rerio* histone deacetylase 6 catalytic domain 2 in complex with ACY1215 was used as the template (PDB code: 5WGL). From the proposed binding mode, we can see that the hydroxamic acid group of both compounds can smoothly chelate with the  $Zn^{2+}$  which makes contribution for the HDAC6 inhibition. For compound MH1-18 (Figure 3A), the oxygen atom of the terminal carboxyl group forms a hydrogen bond with Arg636 residue of HDAC6. While for compound MH1-21 (Figure 3B), the oxygen atom of the carboxyl group forms an extra hydrogen bond with Ser531 residue of HDAC6, and a  $\pi$ - $\pi$  stack interaction is predicted to be formed between the triazole and the phenyl group of Phe643 residue.

## 4. Conclusion

In this work, a series of 21 novel HDAC inhibitors possessing 4-piperidin-4-yl- triazole as the core skeleton were rationally designed based on the pharmacophore constituents of known HDACis. All of the target compounds displayed moderate to excellent inhibitory activity to HDACs. Out of them, compounds MH1-18 and MH1-21 with inhibition rate exceeding 90% toward HDACs at 1  $\mu$ M exhibited potent inhibitory activity toward HDAC6 isoform, and MH1-21 displayed good selectivity to HDAC6 over HDAC1, better than

ACY1215. In addition, compound MH1-21 showed potent efficacy in suppressing the migration of MCF-7 cells *in vitro*. Compounds obtained in the current study shed light on discovering novel HDAC6 inhibitors as anti-cancer agents.

## Acknowledgements

We gratefully acknowledge the financial support from the National Science Foundation for Young Scientists of China to Y. L. (NSFC no. 81602947) and J. G. (NSFC no. 81503094), China Postdoctoral Science Foundation (no. 2016M600524), and Qingdao Postdoctoral Applied Research Project (no. 2016072; Jianjun Gao, Qingdao University).

## References

1. Minucci S, Pelicci PG. Histone deacetylase inhibitors and the promise of epigenetic (and more) treatments for cancer. *Nat Rev Cancer*. 2006; 6:38-51.
2. de Ruijter AJ, van Gennip AH, Caron HN, Kemp S, van Kuilenburg AB. Histone deacetylases (HDACs): characterization of the classical HDAC family. *Biochem J*. 2003; 370:737-749.
3. Gregoret IV, Lee YM, Goodson HV. Molecular evolution of the histone deacetylase family: functional implications of phylogenetic analysis. *J Mol Biol*. 2004; 338:17-31.
4. Kalin JH, Bergman JA. Development and therapeutic implications of selective histone deacetylase 6 inhibitors. *J Med Chem*. 2013; 56:6297-6313.
5. Falkenberg KJ, Johnstone RW. Histone deacetylases and their inhibitors in cancer, neurological diseases and immune disorders. *Nat Rev Drug Discov*. 2014; 13:673-691.
6. Khan O, La Thangue NB. HDAC inhibitors in cancer biology: emerging mechanisms and clinical applications. *Immunol Cell Biol*. 2012; 90:85-94.

7. Gammoh N, Lam D, Puente C, Ganley I, Marks PA, Jiang X. Role of autophagy in histone deacetylase inhibitor-induced apoptotic and nonapoptotic cell death. *Proc Natl Acad Sci U S A*. 2012; 109:6561-6565.
8. Weichert W. HDAC expression and clinical prognosis in human malignancies. *Cancer Lett*. 2009; 280:168-176.
9. Bolden JE, Peart MJ, Johnstone RW. Anticancer activities of histone deacetylase inhibitors. *Nat Rev Drug Discov*. 2006; 5:769-784.
10. Thaler F, Mercurio C. Towards selective inhibition of histone deacetylase isoforms: what has been achieved, where we are and what will be next. *Chem Med Chem*. 2014; 9:523-526.
11. Wagner JM, Hackanson B, Lubbert M, Jung M. Histone deacetylase (HDAC) inhibitors in recent clinical trials for cancer therapy. *Clin Epigenetics*. 2010; 1:117-136.
12. Lu X, Ning Z, Li Z, Cao H, Wang X. Development of chidamide for peripheral T-cell lymphoma, the first orphan drug approved in China. *Intractable Rare Dis Res*. 2016; 5:185-191.
13. Ramalingam SS, Belani CP, Ruel C, Frankel P, Gitlitz B, Koczywas M, Espinoza-Delgado I, Gandara D. Phase II study of belinostat (PXD101), a histone deacetylase inhibitor, for second line therapy of advanced malignant pleural mesothelioma. *J Thorac Oncol*. 2009; 4:97-101.
14. Bumber Y, Younes A, Garcia-Manero G. Mocetinostat (MGCD0103): a review of an isotype-specific histone deacetylase inhibitor. *Expert Opin Investig Drugs*. 2011; 20:823-829.
15. Fraczek J, Vanhaecke T, Rogiers V. Toxicological and metabolic considerations for histone deacetylase inhibitors. *Expert Opin Drug Metab Toxicol*. 2013; 9:441-457.
16. Dallavalle S, Pisano C, Zunino F. Development and therapeutic impact of HDAC6-selective inhibitors. *Biochem Pharmacol*. 2012; 84:756-765.
17. Zuo Q, Wu W, Li X, Zhao L, Chen W. HDAC6 and SIRT2 promote bladder cancer cell migration and invasion by targeting cortactin. *Oncol Rep*. 2012; 27:819-824.
18. Hideshima T, Bradner JE, Chauhan D, Anderson KC. Intracellular protein degradation and its therapeutic implications. *Clin Cancer Res*. 2005; 11:8530-8533.
19. Li Y, Shin D, Kwon SH. Histone deacetylase 6 plays a role as a distinct regulator of diverse cellular processes. *FEBS J*. 2013; 280:775-793.
20. Zhao C, Gao J, Zhang L, Su L, Luan Y. Novel HDAC6 selective inhibitors with 4-aminopiperidine-1-carboxamide as the core structure enhanced growth inhibitory activity of bortezomib in MCF-7 cells. *Biosci Trends*. 2019; 13:91-97.
21. Santo L, Hideshima T, Kung AL, *et al*. Preclinical activity, pharmacodynamic, and pharmacokinetic properties of a selective HDAC6 inhibitor, ACY-1215, in combination with bortezomib in multiple myeloma. *Blood*. 2012; 119:2579-2589.
22. Haggarty SJ, Koeller KM, Wong JC, Grozinger CM, Schreiber SL. Domain-selective small-molecule inhibitor of histone deacetylase 6 (HDAC6)-mediated tubulin deacetylation. *Proc Natl Acad Sci U S A*. 2003; 100:4389-4394.
23. Haggarty SJ, Koeller KM, Wong JC, Butcher RA, Schreiber SL. Multidimensional chemical genetic analysis of diversity-oriented synthesis-derived deacetylase inhibitors using cell-based assays. *Chem Biol*. 2003; 10:383-396.
24. Sun Z, Zhu Y, Aminbuhe, Fan Q, Peng J, Zhang N. Differential expression of APE1 in hepatocellular carcinoma and the effects on proliferation and apoptosis of cancer cells. *Biosci Trends*. 2018; 12:456-462.
25. Yang Z, Ji L, Jiang G, Liu R, Liu Z, Yang Y, Ma Q, Zhao H. FL118, a novel camptothecin analogue, suppressed migration and invasion of human breast cancer cells by inhibiting epithelial-mesenchymal transition via the Wnt/beta-catenin signaling pathway. *Biosci Trends*. 2018; 12:40-46.
26. Zhang X, Li P, Guo S, Wang S, Liu D. Quantitation of beta-carboline and quercetin in alligator weed (*Alternanthera philoxeroides* (Mart.) Griseb.) by LC-MS/MS and evaluation of cardioprotective effects of the methanol extracts. *Drug Discov Ther*. 2018; 12:341-346.
27. Zhang H, Li X, Wang X, Xu W, Zhang J. Sulfonyl phosphonic 1,4-dithia-7-azaspiro[4,4]nonane derivatives as matrix metalloproteinase inhibitors: Synthesis, a docking study, and biological evaluation. *Drug Discov Ther*. 2017; 11:118-125.
28. Marson CM. Histone deacetylase inhibitors: design, structure-activity relationships and therapeutic implications for cancer. *Anticancer Agents Med Chem*. 2009; 9:661-692.
29. Tron GC, Pirali T, Billington RA, Canonico PL, Sorba G, Genazzani AA. Click chemistry reactions in medicinal chemistry: applications of the 1,3-dipolar cycloaddition between azides and alkynes. *Med Res Rev*. 2008; 28:278-308.
30. Wang XN, Wang KY, Zhang XS, Yang C, Li XY. 4-Hydroxybenzoic acid (4-HBA) enhances the sensitivity of human breast cancer cells to adriamycin as a specific HDAC6 inhibitor by promoting HIPK2/p53 pathway. *Biochem Biophys Res Commun*. 2018; 504:812-819.
31. Hsieh YL, Tu HJ, Pan SL, Liou JP, Yang CR. Antimetastatic activity of MPT0G211, a novel HDAC6 inhibitor, in human breast cancer cells *in vitro* and *in vivo*. *Biochim Biophys Acta Mol Cell Res*. 2019; 1866:992-1003.

(Received March 2, 2019; Revised April 17, 2019; Accepted April 21, 2019)